Ind. J. Pharm. Edu. Res., 2027; 1-6.
https://www.ijper.org

Original Article

Interaction Study of Natural Compounds Against NSP15 of SARS-COV-2 Virus

Congling Chen[1], Zhanxiang Wang[2], Sixue Zhang[3,*]

[1]Department of Respiratory and Critical Care Medicine, Chang'an Hospital, Xi'an, CHINA.
[2]Department of Emergency Medicine, Chang'an Hospital Xi'an, CHINA.
[3]Department of Geriatric Respiratory Medicine, Xi'an No.1 Hospital, Xi'an, CHINA.

ABSTRACT

Objectives: Mutations in the SARS-CoV-2 virus and cases of reinfection post-vaccination across multiple countries have intensified the search for effective antiviral treatments. Naturally derived medicinal compounds are being explored as promising alternatives for treating COVID-19. Nonstructural Protein 15 (NSP15) plays a critical role in viral replication and immune evasion, making it a potential therapeutic target. **Materials and Methods:** This study utilized bio-computational approaches to screen various biogenic compounds for their potential to inhibit the catalytic site of SARS-CoV-2 NSP15. After performing detailed molecular docking analyses on top-ranked candidates, a virtual screening of a biogenic compound library from the ZINC database was carried out. Molecular dynamics simulations were conducted using GROMACS version 2020.2 with the GROMOS53a6 force field, where the protein was solvated in a dodecahedron box with SPC216 water, followed by energy minimization and equilibration at 300 K for 1 ns, before a 50 ns production run, with ligand topology prepared via the PRODRG server. **Results:** The compound ZINC14641675 emerged as a strong candidate, demonstrating stability within the NSP15 active site during molecular dynamics simulations. **Conclusion:** The findings suggest that further research and validation of this compound could contribute to the development of an effective treatment for SARS-CoV-2.

Keywords: Natural compound, SARS-CoV-2 therapy, ZINC database, NSP15.

Correspondence:
Dr. Sixue Zhang
Department of Geriatric Respiratory Medicine Xi'an No.1 Hospital Xi'an 710000 CHINA.
Email: zhangsixue2003@sina.com

www.ijper.org

INTRODUCTION

The COVID-19 pandemic is caused by Severe Acute Respiratory Syndrome Coronavirus 2 (SARS-CoV-2). Characterizing the biology and improving multiple diagnosis and treatment options, varying through vaccines to antibodies to antivirals, have been the focus of concerted efforts and hot area of the research. Researchers from all around the world are working tirelessly to discover novel COVID-19 therapies and interventions, with different clinical trials starting almost every day.[1] Antivirals, which prevent the virus from spreading, and immune modulators are the two major forms of COVID-19 therapies that are currently being used.[2] Over a thousand drugs are already in the COVID-19 therapeutic pipeline, the majority of which are still in the development stage, and many of which are already approved drugs for other diseases that are being tested for SARS-CoV-2.

DOI: 10.5530/ijper.20272985

Copyright Information :
Copyright Author (s) 2027 Distributed under Creative Commons CC-BY 4.0

Publishing Partner : Manuscript Technomedia. [www.mstechnomedia.com]

WHO has listed four vaccines for emergency use as of April 12, 2021.[3] As an urgent consequence of the novelty of SARS-CoV-2 infections and the lack of effective drugs, a wide range of techniques and methods are being used to tackle the emerging worldwide COVID-19 pandemic.

Nonstructural Viral Proteins (NSPs) are among the druggable targets of SARS-CoV-2 on the list of critical targets. The genomic content of SARS-CoV-2 is 70%-80% like SARS-CoV.[4] The NSP15 protein of SARS-CoV-2 is 89% identical to the SARS-CoV protein. Studies have shown that inhibition of NSP15 can slow down viral replication.[5] This implies that drugs targeting NSP15 could be produced as useful anti-COVID-19 drugs.[3] Recent advancements in COVID-19 therapies have focused on various targets, with NSP15 emerging as a promising candidate due to its role in viral replication and immune evasion. NSP15, a non-structural protein of SARS-CoV-2, has been identified as crucial for the virus's ability to evade host immune responses by cleaving viral RNA and modulating the host's innate immune response. Current research has explored inhibitors targeting NSP15, demonstrating potential in disrupting viral replication and enhancing antiviral efficacy.[5] Additionally, the development of small-molecule inhibitors and monoclonal antibodies targeting NSP15 is being investigated as part of a broader strategy to combat COVID-19, particularly in

light of evolving variants. These efforts highlight the significance of NSP15 in therapeutic strategies and underscore the need for continued research into its role in COVID-19 pathogenesis.

Natural products and their structural analogues have long been important in pharmacotherapy, particularly in the treatment of cancer and infectious diseases. Natural products are typically easier to digest than synthetic substances and are generally non-toxic.[6] Surprisingly, it is estimated that about half of the pharmaceuticals actually in use are made from natural ingredients.[7] Nature has a huge list of chemicals that are yet to be investigated and developed into medications to cure various viral illnesses. Few natural products have been found to have antiviral activity in nanomolar concentrations contributing to further drug development.[8]

The computational approaches are predictive and provide an indication of the potency of a molecule/compound. *In silico* drugs have emerged as a result of advances in bio-computational research over the last few decades. In this study, we conducted structure-based virtual screening against the active site of NSP-15, as well as in-depth docking and Molecular Dynamics (MD) studies on the best-scored natural compound, which could prove to be a possible lead molecule after subsequent experimental validation.

MATERIALS AND METHODS

Preparations of target protein and ligand molecules

The crystal structure of NSP15 endoribonuclease from SARS CoV-2 was downloaded from the Protein Data Bank (PDB ID: 6VWW) with 2.20 Å resolution.[9] Water and co-crystalized ligands were removed, and the monomer protein was then energy-minimized using Chimera.[10]

Biogenic compounds were retrieved from the ZINC database.[11] by narrowing the search to "in-vitro-only and biogenic" as the subsets that included biogenic compounds that were active at 10 uM or higher in direct binding assays. A total of 90164 biogenic compounds were extracted, which were then subjected to minimization and ligand preparation process using Discover Studio 2020's ligand preparation method.

Structure-Based Virtual Screening (SBVS)

SBVS is a technique used in drug development and discovery to search the novel bioactive molecules against a target.[12] The prepared biogenic compound library was screened against the 6VWW catalytic site. It was carried out with the aid of Autodock Vina.[13] In the present study, we explored the best scoring molecule (ZINC14641675) by further in-depth molecular docking interaction and molecular dynamics simulation.

Molecular interaction

To compute the binding affinity of the ZINC14641675, the half-maximal inhibitory concentration (IC_{50}) against NSP15 was predicted using Autodock tools.[14] The grid box spacing was 0.375 Å.[15] The number of individuals in the population and the maximum number of energy evaluations in each run was kept 150 and 25,000,000, respectively to determine the best docking conformer, and other docking parameters were set to default. Overall, 10 conformations of the compound were generated with IC_{50} values. Finally, ZINC14641675 complexes with NSP15 was used for MD simulation.

In silico pharmacokinetics analysis

SwissADME (version 2025) was used to analyze the pharmacokinetics properties of finally screened compound.[16] Lipinski's criteria were also evaluated for a compound to exhibit drug likeness, the criteria to be fulfilled are molecular weight <500 Daltons, calculated lipophilicity (Log P) <5, number of hydrogen-bond acceptors <10, and number of hydrogen-bond donors <5.[17] Using the same software, the solubility (Log S) for absorption and bioavailability was also predicted. As previously elucidated, values of Log S equivalent or greater than -4 is revealing the favorable solubility.[18]

Molecular dynamics simulation system preparation

GROMACS version 2020.2 packages were used for preparing the system and performing MD simulations using the gromos53a6 force field.[19,20] The protein solute was solvated by explicit SPC216 water[21] in a dodecahedron box with a margin of 10 Å between solute and the box walls. The LINCS algorithm of fourth-order expansion was used to constrain bond lengths.[22] The steepest-descent algorithm was applied to optimize for 10 000 steps to remove steric clashes between atoms. The system was equilibrated for 1 ns with position restraints of all heavy atoms. Berendsen weak coupling schemes were used to maintain the system at 300 K and 1 atom using separate baths for the system. Initial velocities were generated randomly using a Maxwell-Boltzmann distribution corresponding to 300 K. Finally, the production run was performed for total 50 ns. Furthermore, xmgrace (http://plasma-gate.weizmann.ac.il) was used for preparing graphs. Ligand topology preparation was implemented by using the PRODRG server with the option of choosing no chirality, full charge and no energy minimization.[23]

www.ijper.org

Table 1: ADME/Tox properties of ZINC14641675.

Property	Parameters	ZINC14641675
Absorption	Water solubility (log mol/L))	-3.177
	Caco2 permeability (log Papp in 10-6 cm/s)	0.57
	Intestinal absorption (human) (% Absorbed)	69.99
	Skin Permeability (log Kp)	-2.735
	P-glycoprotein substrate (Yes/No)	Yes
	P-glycoprotein I inhibitor (Yes/No)	Yes
	P-glycoprotein II inhibitor (Yes/No)	Yes
Distribution	VDss (human) (log L/kg)	-0.001
	Fraction unbound (human) (Fu)	0.212
	BBB permeability (log BB)	-1.297
	CNS permeability (log PS)	-2.743
Metabolism	CYP2D6 substrate (Yes/No)	No
	CYP3A4 substrate (Yes/No)	No
	CYP1A2 inhibitor (Yes/No)	No
	CYP2C19 inhibitor (Yes/No)	Yes
	CYP2C9 inhibitor (Yes/No)	Yes
	CYP2D6 inhibitor (Yes/No)	No
	CYP3A4 inhibitor (Yes/No)	No
Excretion	Total Clearance (log mL/min/kg)	0.681
	Renal OCT2 substrate (Yes/No)	No
Toxicity	AMES toxicity (Yes/No)	No
	Max. tolerated dose (human) (log mg/kg/day)	0.566
	hERG I inhibitor (Yes/No)	No
	hERG II inhibitor (Yes/No)	Yes
	Oral Rat Acute Toxicity (LD50) (mol/kg)	2.691
	Oral Rat Chronic Toxicity (LOAEL) (log mg/kg/bw/day)	2.467
	Hepatotoxicity (Yes/No)	No
	Skin Sensitization (Yes/No)	No
	T. Pyriformis toxicity (log ug/L)	0.286
	Minnow toxicity (log mM)	-0.515

RESULTS AND DISCUSSION

The fast transmissibility and the deficiency of specific drugs against the COVID-19 disease encouraged the virtual screening of phytochemicals to identify the best lead compounds. In this study, we chose NSP15 as a target molecule that has been identified as one of the most druggable targets in the literature.[24] We choose the most studied and first released x-ray structure (6vww) for this study out of 19 x-ray crystal structures and 1 cryo-EM structure present in the PDB. The prepared library of biogenic compounds was screened against the 6vww catalytic site using the x, y, and z centers of 69.377, 26.349, and 34.546, respectively.

Finally, we find ZINC14641675, which was showing good ADME/Tox properties (Table 1) and Lipinski rule. The selected ligand was following the nearly all the rule for druglikeness as shown in Table 2.

ZINC14641675 was found to interact with 6vww with fourteen amino acid residues like GLU69, LYS71, LYS90, GLY165, VAL166, THR167, ILE169, SER198, ARG199, ASN200, GLU203, PHE204, LYS205, and ARG207. Among these amino acid residues namely, LYS90, GLY165, VAL166, THR167, SER198, ARG199, and ASN200 was reported into the interaction of Arzanol with NSP15[25] which is interestingly found in this study.

www.ijper.org

Table 2: The physicochemical properties of the selected compound ZINC14641675.

Properties		ZINC14641675
Physicochemical properties	Formula	$C_{26}H_{32}O_6$
	Molecular weight (g/mol)	440.53
	H-bond acceptors	6
	H-bond donors	4
	TPSA (Å^2)	107.22
Pharmacokinetics	GI absorption	High
Druglikeness	Lipinski Rule	Yes
	Ghose Rule	Yes
	Veber Rule	Yes
	Egan Rule	Yes
	Muegge Rule	No; 1 violation: XLOGP3>5

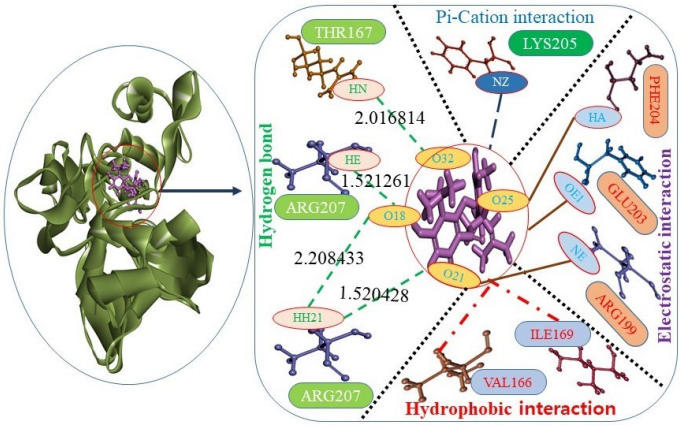


Figure 1: Molecular interaction of selected compound with NSP15. Green line represents the amino acid residues involved in H-bond interaction. Red line represents the amino acid residues involved in hydrophobic interaction. Brown line represents the amino acid residues involved in electrostatic interaction. Blue line represents the amino acid residues involved in Pi-cation interaction.

The different types of chemical bonds were formed upon the binding of the ZINC14641675 with the active site of the NSP15. These bonds are hydrogen bonds, hydrophobic interactions, pi-cation bond, and electrostatic interaction. It is well known that the receptor has lost its functional enzymatic activity upon the blocked of the active site. This inhibition approach was adopted in this study to find novel inhibitors for SARS-CoV-2 by inhibiting NSP15.

Besides these four H-bond interactions was found in the complex formation of 'NSP15- ZINC14641675'. These H-bonds are namely, THR167:HN - UNK0:O32, ARG207: HE - UNK0:O18, ARG207:HH21 - UNK0:O18, and ARG207:HH21

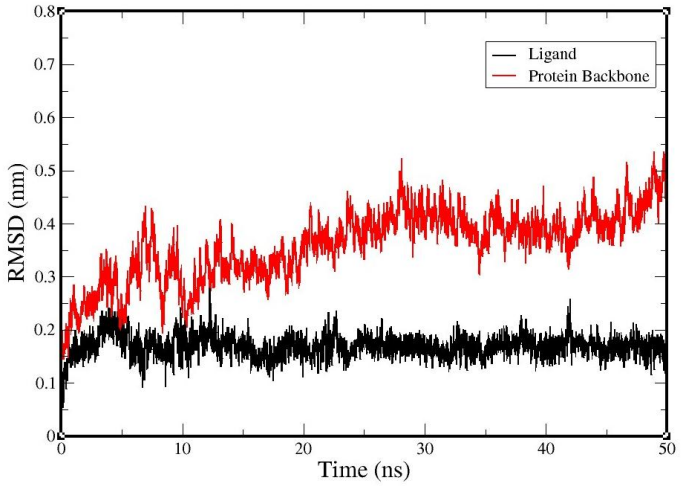


Figure 2: RMSD plot for ligand within the close contact residues of protein.

- UNK0:O21 along with H-bond distances 2.016814, 1.521261, 2.208433, and 1.520428 Å respectively. Two amino acid residues VAL166 and ILE169 were found to be involved in hydrophobic interaction in the positioning of ligand to the active site of target namely, VAL166 -: UNK0 and UNK0 - A: ILE169. In the interaction of ligand to the target, three amino acid residues ARG199, GLU203, and PHE204 were found into the electrostatic interaction like, ARG199:NE - UNK0:O21, GLU203:OE1 - UNK0 and PHE204: HA - UNK0:O25 respectively. All these interactions are shown in Figure 1. Besides these interactions, one pi-cation interaction was found as LYS205:NZ – UNK0. Among these bonds, H-bonds play an important role in protein-ligand interaction and lower the binding energy to stabilize the docked complex.[26–28] The intermolecular energy of docking for 'NSP15-ZINC14641675' interaction was found to be -8.24 kcal/mol. 'Van der Waals', 'H-Bond' and 'desolvation' energy components together contributed -8.0 kcal/mol while the 'Electrostatic' energy components were found to be -0.24 kcal/mol. The selected compound (ZINC14641675) is following the Lipinski's rule of five. This compound has high gastrointestinal absorption.[16] Likewise, this selected compound is following the Lipinski et al. (2001), Ghose et al. (1999) rule, Veber et al. (2002) rule, and Egan et al. (2000) rule shown in Table 2.[29–32]

Root Mean Square Deviation (RMSD)

The stability of the trajectories was calculated by the Root Mean Square Deviation (RMSD). Figure 2 reports the RMSD of the backbone atoms for the trajectory. RMSD changes in all the systems were initiated at the same point which was noted as ~0.15 nm. The red line represents the RMSD values change in protein complex that indicates a bit fluctuation till ~30ns and after this time, RMSDs found stable which remain plateau and average value was noted as 0.395nm.

www.ijper.org

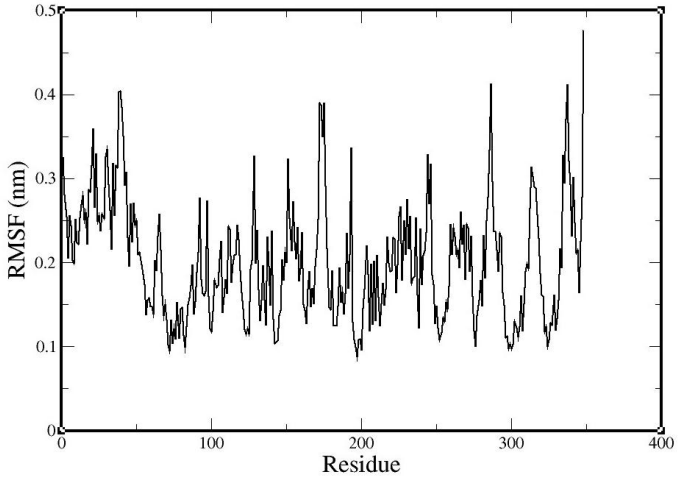


Figure 3: Graphical representation of RMSF by considering protein backbone. Higher and lower picks exhibit greater and lesser flexibility respectively in particular residues.

Whereas, RMSD plot of ligand (black) was shown sudden elevation at very initial time and the starts on ~0.05nm, beginning and it was found highly fluctuations till 10ns. However, the RMSD values maintain plateau after ~10ns and average value noted was 0.18 nm. Consequently, RMSDs were found stable and robust trajectories during simulation. Although the simulation was for 50 ns, the discrepancy from the initial structure within the first 25 ns was sufficient to point out the protein structures, that were substantially denatured at binding sites and adjacent area.

Moreover, RMSDs of ligand candidates were also calculated to evaluate the behavior of ligands within binding site of protein. Figure 2 reports the plot representation of RMSD for selected ligand. Ligand was showing high stability within the close contact residues of protein. However, the average RMSD of ligand was noted 0.127 nm and lied approximately 0.05nm to 0.2nm during the simulation.

Root-Mean Square Fluctuations (RMSF)

Residues of N- and C-terminal for RMSF calculations were ignored and the maximum RMSF value for simulation reported here is ~0.41 nm of GLN286 residues which was detected in neighbor residues from the active site. In addition, GLY39, GLU172, ALA173, VAL174, LYS175 and ASP337 were found particularly with higher flexibility. Considering range in residues 90-340 was employed in the width of high RMSF peak (Figure 3). The corresponding pattern was expressed to be in good agreement with the secondary structure and with the B-factors reported for the initial structure.

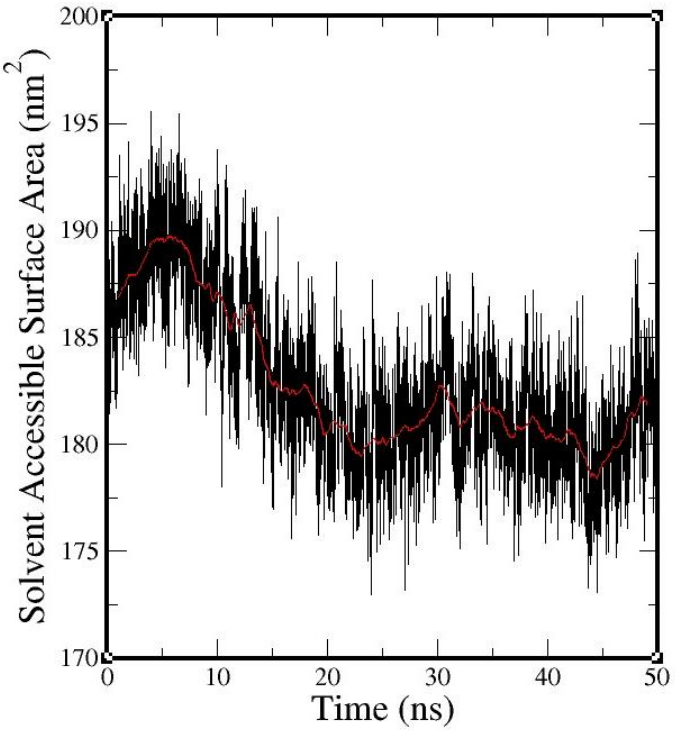


Figure 4: Representation of Solvent Accessible Surface Area (SASA) over the simulation of protein complex.

Solvent Accessible Surface Area (SASA)

To deduce the conformational changes and area occupied by water molecule, SASA was approximated and changes at simulation time were monitored (Figure 4). Considering protein backbone for calculation of SASA, sudden increments are examined within time of ~8 ns and the average value found as ~192.5 nm2, and later continuously declined and reached ~180 nm2 at time of ~15 ns. From the highest point, a considerable decrease in SASA was observed.

CONCLUSION

This study highlights the potential of ZINC14641675 as a promising inhibitor of SARS-CoV-2 Nonstructural Protein 15 (NSP15), which plays a crucial role in viral replication and immune evasion. Through a comprehensive bio-computational approach, we demonstrated that ZINC14641675 exhibits strong binding affinity and stability within the NSP15 active site, supported by molecular dynamics simulations. The compound adheres to established drug-likeness criteria, indicating its suitability for further development as a therapeutic agent against COVID-19. The findings underscore the importance of exploring naturally derived compounds as viable alternatives in the ongoing search for effective antiviral treatments. Future experimental validation of ZINC14641675, along with further optimization and characterization, could pave the way for its potential application in clinical settings. Continued research into the interactions

www.ijper.org

between NSP15 and biogenic compounds will enhance our understanding of antiviral mechanisms and contribute to the development of targeted therapies for COVID-19 and other related viral infections.

CONFLICT OF INTEREST

The authors declare that there is no conflict of interest.

ETHICAL APPROVAL

The experimental protocols of this study were approved by Xi'an No.1 Hospital.

REFERENCES

1. Zhang T, Wu Q, Zhang Z. Probable Pangolin Origin of SARS-CoV-2 Associated with the COVID-19 Outbreak. *Curr Biol.* 2020;30:1578. doi:10.1016/j.cub.2020.03.063.
2. Dube T, Ghosh A, Mishra J, Kompella UB, Panda JJ. Repurposed Drugs, Molecular Vaccines, Immune-Modulators, and Nanotherapeutics to Treat and Prevent COVID-19 Associated with SARS-CoV-2, a Deadly Nanovector. *Advanced Therapeutics.* 2020;2000172.
3. Doshi RH. COVID-19 Vaccination Coverage—World Health Organization African Region, 2021–2023. *MMWR Morb Mortal Wkly Rep.* 2024;73.
4. Ceccarelli M, Berretta M, Venanzi Rullo E, Nunnari G, Cacopardo B. Differences and similarities between Severe Acute Respiratory Syndrome (SARS)-CoronaVirus (CoV) and SARS-CoV-2. Would a rose by another name smell as sweet? *Eur Rev Med Pharmacol Sci.* 2020;24:2781-2783. doi:10.26355/eurrev_202003_20551.
5. Gao B, Gong X, Fang S, Weng W, Wang H, Chu H, Sun Y, Meng C, Tan L, Song C. Inhibition of anti-viral stress granule formation by coronavirus endoribonuclease NSP15 ensures efficient virus replication. *PLoS Pathog.* 2021;17:e1008690.
6. Atanasov AG, Zotchev SB, Dirsch VM, Supuran CT. Natural products in drug discovery: Advances and opportunities. *Nat Rev Drug Discov.* 2021;1-17.
7. Newman DJ, Cragg GM. Natural products as sources of new drugs from 1981 to 2014. *J Nat Prod.* 2016;79:629-661.
8. Islam MT, Sarkar C, El-Kersh DM, Jamaddar S, Uddin SJ, Shilpi JA, Mubarak MS. Natural products and their derivatives against coronavirus: A review of the non-clinical and pre-clinical data. *Phytother Res.* 2020;34:2471-2492.
9. Kim Y, Jedrzejczak R, Maltseva NI, Wilamowski M, Endres M, Godzik A, Michalska K, Joachimiak A. Crystal structure of NSP15 endoribonuclease NendoU from SARS-CoV-2. *Protein Sci.* 2020;29:1596-1605. doi:10.1002/pro.3873.
10. Pettersen EF, Goddard TD, Huang CC, Couch GS, Greenblatt DM, Meng EC, Ferrin TE. UCSF Chimera—a visualization system for exploratory research and analysis. *J Comput Chem.* 2004;25:1605-1612.
11. Irwin JJ, Sterling T, Mysinger MM, Bolstad ES, Coleman RG. ZINC: a free tool to discover chemistry for biology. *J Chem Inf Model.* 2012;52:1757-1768.
12. Lionta E, Spyrou G, Vassilatis DK, Cournia Z. Structure-based virtual screening for drug discovery: principles, applications and recent advances. *Curr Top Med Chem.* 2014;14:1923-1938.
13. Trott O, Olson AJ. AutoDock Vina: improving the speed and accuracy of docking with a new scoring function, efficient optimization, and multithreading. *J Comput Chem.* 2010;31:455-461. doi:10.1002/jcc.21334.
14. Morris GM, Huey R, Lindstrom W, Sanner MF, Belew RK, Goodsell DS, Olson AJ. AutoDock4 and AutoDockTools4: Automated docking with selective receptor flexibility. *J Comput Chem.* 2009;30:2785-2791. doi:10.1002/jcc.21256.
15. Chandra A, Gurjar V, Qamar I, Singh N. Identification of potential inhibitors of SARS-COV-2 endoribonuclease (EndoU) from FDA approved drugs: a drug repurposing approach to find therapeutics for COVID-19. *J Biomol Struct Dyn.* 2021;39:4201-4211. doi:10.1080/07391102.2020.1775127.
16. Daina A, Michielin O, Zoete V. SwissADME: a free web tool to evaluate pharmacokinetics, drug-likeness and medicinal chemistry friendliness of small molecules. *Sci Rep.* 2017;7:42717. doi:10.1038/srep42717.
17. Lipinski CA. Chris Lipinski discusses life and chemistry after the Rule of Five. *Drug Discov Today.* 2003;8:12-16. doi:10.1016/s1359-6446(02)02556-4.
18. Escobedo-Gonzalez R, Vargas-Requena CL, Moyers-Montoya E, Aceves-Hernandez JM, Nicolas-Vazquez MI, Miranda-Ruvalcaba R. *In silico* Study of the Pharmacologic Properties and Cytotoxicity Pathways in Cancer Cells of Various Indolylquinone Analogues of Perezone. *Molecules.* 2017;22. doi:10.3390/molecules22071060.
19. Pronk S, Pall S, Schulz R, Larsson P, Bjelkmar P, Apostolov R, Shirts MR, Smith JC, Kasson PM, van der Spoel D, et al. GROMACS 4.5: a high-throughput and highly parallel open source molecular simulation toolkit. *Bioinformatics.* 2013;29:845-854. doi:10.1093/bioinformatics/btt055.
20. Van Der Spoel D, Lindahl E, Hess B, Groenhof G, Mark AE, Berendsen HJ. GROMACS: fast, flexible, and free. *J Comput Chem.* 2005;26:1701-1718. doi:10.1002/jcc.20291.
21. Oostenbrink C, Villa A, Mark AE, van Gunsteren WF. A biomolecular force field based on the free enthalpy of hydration and solvation: the GROMOS force-field parameter sets 53A5 and 53A6. *J Comput Chem.* 2004;25:1656-1676. doi:10.1002/jcc.20090.
22. Hess B, Bekker H, Berendsen HJ, Fraaije JG. LINCS: a linear constraint solver for molecular simulations. *J Comput Chem.* 1997;18:1463-1472.
23. Schuttelkopf AW, van Aalten DM. PRODRG: a tool for high-throughput crystallography of protein-ligand complexes. *Acta Crystallogr D Biol Crystallogr.* 2004;60:1355-1363. doi:10.1107/S0907444904011679.
24. Zhang L, Li L, Yan L, Ming Z, Jia Z, Lou Z, Rao Z. Structural and Biochemical Characterization of Endoribonuclease NSP15 Encoded by Middle East Respiratory Syndrome Coronavirus. *J Virol.* 2018;92. doi:10.1128/JVI.00893-18.
25. Salman S, Shah FH, Idrees J, Idrees F, Velagala S, Ali J, Khan AA. Virtual screening of immunomodulatory medicinal compounds as promising anti-SARS-COV-2 inhibitors. *Future Virology.* 2020;15:267-275.
26. Patil R, Das S, Stanley A, Yadav L, Sudhakar A, Varma AK. Optimized hydrophobic interactions and hydrogen bonding at the target-ligand interface leads the pathways of drug-designing. *PLoS One.* 2010;5:e12029. doi:10.1371/journal.pone.0012029.
27. Ahmad SS, Khan H, Danish Rizvi SM, Ansari SA, Ullah R, Rastrelli L, Mahmood HM, Siddiqui MH. Computational Study of Natural Compounds for the Clearance of Amyloid-Betaeta: A Potential Therapeutic Management Strategy for Alzheimer's Disease. *Molecules.* 2019;24. doi:10.3390/molecules24183233.
28. Ahmad SS, Sinha M, Ahmad K, Khalid M, Choi I. Study of Caspase 8 Inhibition for the Management of Alzheimer's Disease: A Molecular Docking and Dynamics Simulation. *Molecules.* 2020;25. doi:10.3390/molecules25092071.
29. Lipinski CA, Lombardo F, Dominy BW, Feeney PJ. Experimental and computational approaches to estimate solubility and permeability in drug discovery and development settings. *Adv Drug Deliv Rev.* 2001;46:3-26. doi:10.1016/s0169-409x(00)00129-0.
30. Ghose AK, Viswanadhan VN, Wendoloski JJ. A knowledge-based approach in designing combinatorial or medicinal chemistry libraries for drug discovery. 1. A qualitative and quantitative characterization of known drug databases. *J Comb Chem.* 1999;1:55-68. doi:10.1021/cc9800071.
31. Veber DF, Johnson SR, Cheng HY, Smith BR, Ward KW, Kopple KD. Molecular properties that influence the oral bioavailability of drug candidates. *J Med Chem.* 2002;45:2615-2623. doi:10.1021/jm020017n.
32. Egan WJ, Merz KM Jr, Baldwin JJ. Prediction of drug absorption using multivariate statistics. *J Med Chem.* 2000;43:3867-3877. doi:10.1021/jm000292e.

Cite this article: Chen C, Wang Z, Zhang S. Interaction Study of Natural Compounds Against NSP15 of SARS-COV-2 Virus. Indian J of Pharmaceutical Education and Research. 2027;1-6.

www.ijper.org